

Article

Optical Resolution of Dimethyl α -Hydroxy-Arylmethylphosphonates via Diastereomer Complex Formation Using Calcium Hydrogen *O,O'*-Dibenzoyl-(2*R*,3*R*)-Tartrate; X-Ray Analysis of the Complexes and Products

Zita Rádai ¹, Péter Bagi ¹, Mátyás Czugler ¹ , Konstantin Karaghiosoff ² 
and György Keglevich ^{1,*} 

¹ Department of Organic Chemistry and Technology, Budapest University of Technology and Economics, 1111 Budapest, Hungary; zradai@gmail.com (Z.R.); peter.bagi@gmx.com (P.B.); mczugler@mail.bme.hu (M.C.)

² Department of Chemie und Biochemie, Ludwig Maximilians Universität, 81377 München, Germany; klk@cup.uni-muenchen.de

* Correspondence: gkeglevich@mail.bme.hu

Received: 1 April 2020; Accepted: 28 April 2020; Published: 6 May 2020



Abstract: Two dimethyl α -hydroxy-arylmethylphosphonates (aryl = Ph and 2-MeOPh) were subjected to optical resolution via diastereomer complex formation applying the acidic calcium salt of *O,O'*-dibenzoyl-(2*R*,3*R*)-tartaric acid as the resolving agent. The dominating diastereomer complexes, whose structure was determined by single crystal X-ray measurements, were obtained in 96% and 68% diastereomer excess values, respectively. After decomposing the diastereomer formations by extraction, and after recrystallizations, the major enantiomer (*S* and *R*, respectively) of the α -hydroxyphosphonates were prepared in enantiomeric excess values of 96% and 68%, respectively. The stereostructure of the two α -hydroxy-arylmethylphosphonates was again established by X-ray measurements. Detailed study on the X-ray data allowed valuable conclusions on the nature of the coordination in the complexes (intermolecular interactions), and on the *H*-bonding.

Keywords: α -hydroxy arylmethylphosphonates; optical resolution; optical isomers; X-ray crystallography; stereostructure; intermolecular interactions; *H*-bonding

1. Introduction

α -Hydroxyphosphonates are important due to their biological activity. Among them there are enzyme inhibitors [1], herbicides [2], bactericides [3], fungicides [4], antioxidants [5], and cytotoxic agents [6,7]. The syntheses of biologically active compounds in enantiopure form is of great importance from the point of view of the pharmaceutical industry, as in most of the cases single enantiomers are the targets [8,9]. For optically active α -hydroxyphosphonates, the main sources have been various enantioselective syntheses [10–12]. The most often used approach is the chiral organocatalyst-assisted addition of dialkyl phosphite to an oxo compound [13–15]. It is also a possibility that metal complexes incorporating chiral ligands are the catalysts [16–19]. Another method involves enantioselective *Abramov*-type condensation of a trialkyl phosphite with a suitable oxo compound [20]. Optically active α -hydroxyphosphonates may also be obtained by asymmetric reduction of α -ketophosphonates [21–23]. Examples for enantioselective oxidation of benzylphosphonates affording α -hydroxyphosphonates are also known [24,25]. As for the optical resolution of α -hydroxyphosphonates, kinetic resolution is the basic method in the literature [26]. This approach usually involves the selective acylation

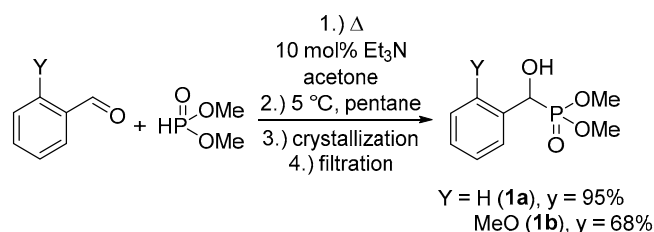
of one enantiomer of the α -hydroxyphosphonate in the presence of an enzyme [27,28] or a chiral organocatalyst [29], leaving the other isomer untouched. Another variant of the optical resolution involves acylation of hydroxyphosphonates with dibenzoyl- (R,R) -tartaric anhydride, that is followed by chromatographic separation, and decomposition of the covalent diastereomers [30]. In our previous article, we reported the synthesis of seven racemic dialkyl 1-hydroxy-arylmethylphosphonates and their structure determined by single crystal X-ray analysis [31]. It was observed that α -hydroxyphosphonates derived from substituted benzaldehydes are inclined to form chain-like associates, while dimers can be found in the crystal lattice of α -hydroxy- α -methylphosphonates formed from acetophenone derivatives [31]. Earlier, we were successful in the optical resolution of a series of cyclic phosphine oxides and phosphinates using the acidic calcium salt of O,O' -dibenzoyl- $(2R,3R)$ -tartaric acid as the resolving agent [32]. It was successfully used for the resolution of tertiary phosphine oxides [33,34], α -alkoxyalcohols [35], α -alkoxycarboxylic acids [36], as well as α - and β -hydroxycarboxylic esters [37] and the biologically active Tenofovir Alafenamide [38].

In this study, we aimed at elaborating the optical resolution of two racemic 1-hydroxy-arylmethylphosphonates via the formation and separation of diastereomeric complexes, and studying the crystal structure of two enantiopure dimethyl 1-hydroxy-arylmethylphosphonates, and their calcium hydrogen O,O' -dibenzoyl- $(2R,3R)$ -tartrate complexes.

2. Results and Discussion

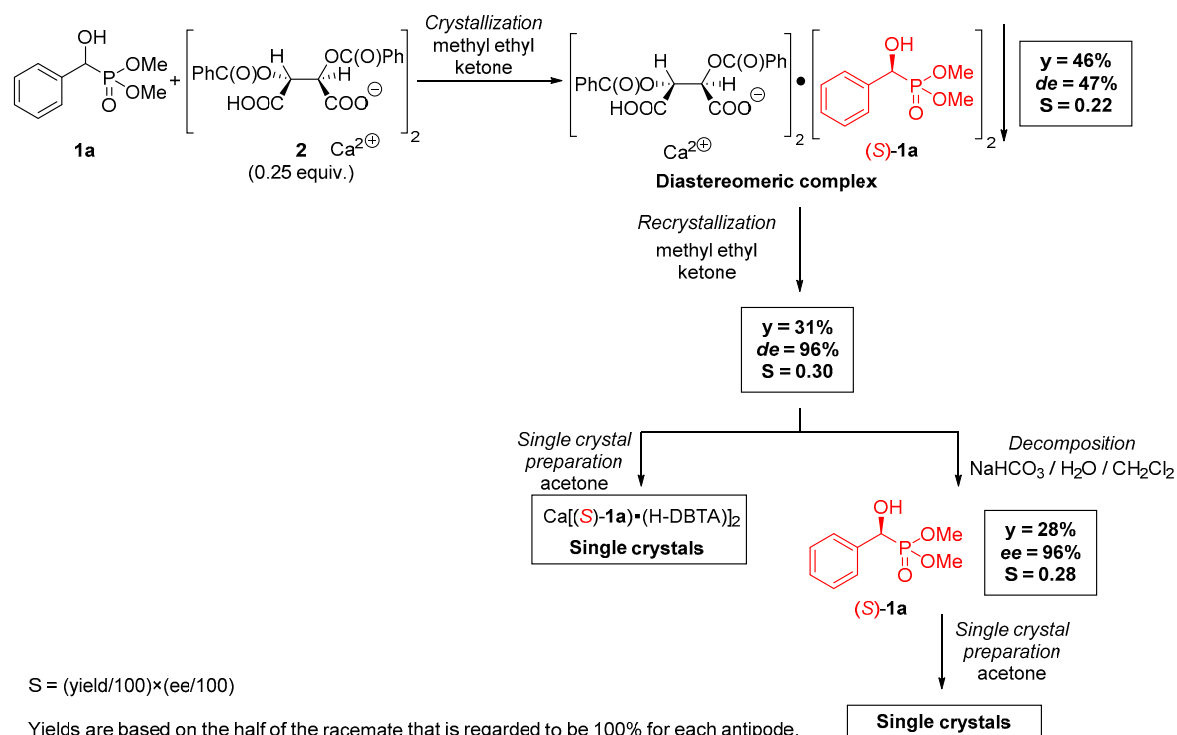
2.1. Preparation of Single Crystals from Optically Active α -Hydroxyphosphonates

At first, racemic α -hydroxybenzyl- and 2-methoxybenzylphosphonates (**1a** and **1b**, respectively) were synthesized according to the method elaborated previously by us (Scheme 1) [39]. The corresponding aromatic aldehyde and dimethyl phosphite were reacted in the presence of triethylamine catalyst in acetone as the solvent. After adding pentane precipitant to the reaction mixture, the racemic product (**1a** or **1b**) crystallized upon cooling, that could be isolated by a simple filtration.



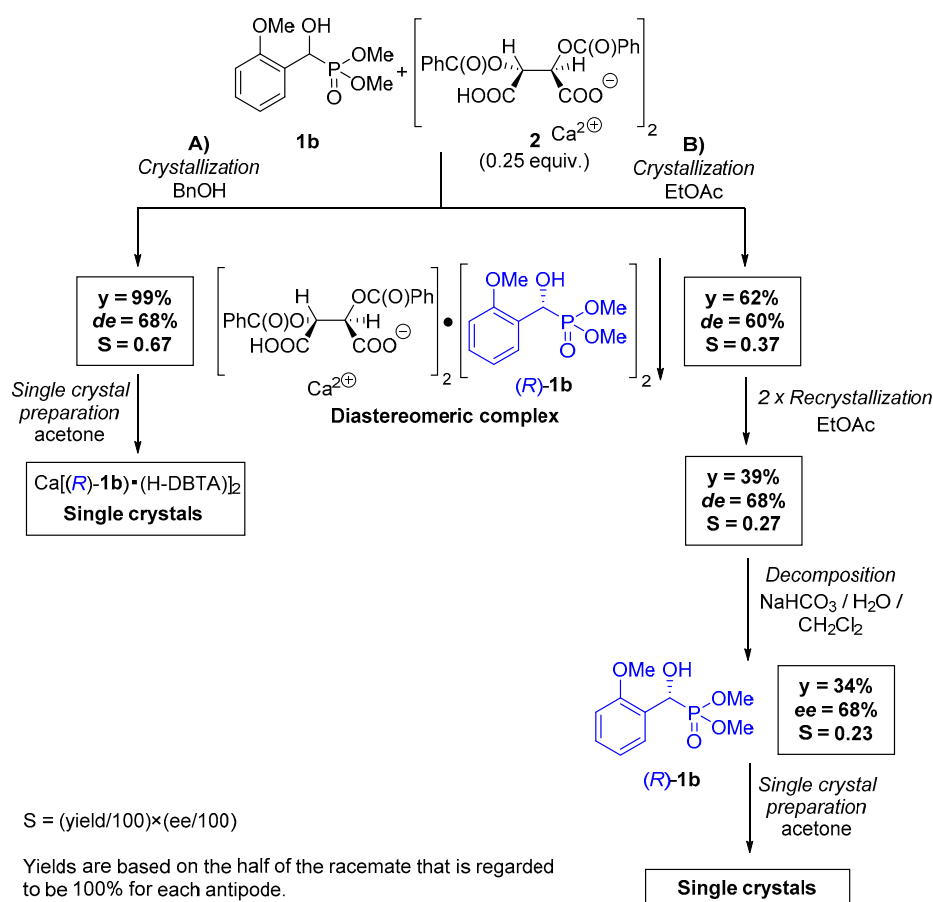
Scheme 1. Synthesis of racemic dimethyl 1-hydroxy-arylmethylphosphonates (**1a** and **1b**).

The acidic calcium salt of O,O' -dibenzoyl- $(2R,3R)$ -tartaric acid ($\text{Ca}(\text{H-DBTA})_2$) (**2**) was used for the resolution of racemic dimethyl 1-hydroxy-arylmethylphosphonates (**1a** and **1b**). Resolving agent $\text{Ca}(\text{H-DBTA})_2$ (**2**) was prepared in the reaction of O,O' -dibenzoyl- $(2R,3R)$ -tartaric acid monohydrate and calcium oxide according to the procedure reported by us [40]. The optical resolution of racemic dimethyl 1-hydroxy-1-phenylmethylphosphonate (**1a**) was carried out using 0.25 equiv. of $\text{Ca}(\text{H-DBTA})_2$ (**2**) in methyl ethyl ketone (Scheme 2). The crystalline diastereomeric complex with a composition of $\text{Ca}[(S)\text{-1a} \bullet \text{H-DBTA}]_2$ was isolated by filtration. The diastereomeric excess of the crystals was 47%, which was determined by chiral HPLC. The diastereomer was purified by recrystallization from methyl ethyl ketone, which afforded $\text{Ca}[(S)\text{-1a} \bullet \text{H-DBTA}]_2$ with a *de* of 96% and in a yield of 31%. Crystals suitable for single crystal X-ray analysis were prepared from this sample by dissolving it in acetone, and allowing the solvent to evaporate slowly. Decomposition of the $\text{Ca}[(S)\text{-1a} \bullet \text{H-DBTA}]_2$ complex by extraction led to an enantiomeric mixture of α -hydroxyphosphonate **1a** with an enantiomeric excess of 96% in yield of 28%. Single crystals of $(S)\text{-1a}$ were prepared from this enantiomeric mixture (Scheme 2).



Scheme 2. Procedure for the resolution of α -hydroxyphosphonate **1a** with $\text{Ca}(\text{H-DBTA})_2$ and the preparation of $\text{Ca}[(\text{S})\text{-1a}] \cdot \text{H-DBTA}_2$ and $(\text{S})\text{-1a}$ single crystals.

The optical resolution of dimethyl 1-hydroxy-1-(2-methoxyphenyl)methylphosphonate (**1b**) was also performed with 0.25 equiv. of $\text{Ca}(\text{H-DBTA})_2$ (**2**) in benzyl alcohol, and also in ethyl acetate (Scheme 3). Using benzyl alcohol as the solvent, the corresponding diastereomeric complex $\text{Ca}[(\text{R})\text{-1b}] \cdot \text{H-DBTA}_2$ was obtained with a diastereomeric excess of 68%, and in yield of 99%. Single crystals were obtained from the diastereomeric complex using acetone as the solvent. The optical resolution of α -hydroxyphosphonate **1b** in ethyl acetate afforded $\text{Ca}[(\text{R})\text{-1b}] \cdot \text{H-DBTA}_2$ with a $de = 60\%$ in a yield of 62%. The diastereomeric complex from the latter experiment was purified by two consecutive recrystallizations from ethyl acetate to give the diastereomer with a de of 68%. The $\text{Ca}[(\text{R})\text{-1b}] \cdot \text{H-DBTA}_2$ complex was decomposed by extraction to give an enantiomeric mixture of α -hydroxyphosphonate $(\text{R})\text{-1b}$ with an enantiomeric excess of 68%, and in a yield of 34%. Single crystals of $(\text{R})\text{-1b}$ were prepared from this enantiomeric mixture using acetone as the solvent (Scheme 3). Despite the fact that diastereomeric or enantiomeric mixtures with an optical purity of 68% (in both cases) were used for the preparation of crystals suitable for X-ray analysis, the corresponding single crystals were of high diastereomer or enantiomer purity ($de/ee > 93\%$). Single crystal X-ray diffraction studies established absolute configurations of the sample crystals of both the resolved target compounds as $(\text{S})\text{-1a}$ and $(\text{R})\text{-1b}$, as well as their complexes $\text{Ca}[(\text{S})\text{-1a}] \cdot \text{H-DBTA}_2$ and $\text{Ca}[(\text{R})\text{-1b}] \cdot \text{H-DBTA}_2$.



Scheme 3. Procedure for the resolution of α -hydroxyphosphonate **1b** with $\text{Ca}(\text{H-DBTA})_2$ and the preparation of $\text{Ca}[(R)\text{-1b}] \cdot \text{H-DBTA}_2$ and $(R)\text{-1b}$ single crystals.

2.2. X-Ray Analysis of Optically Active (*S*)-**1a** and (*R*)-**1b** α -Hydroxyphosphonates and $\text{Ca}[(S)\text{-1a}] \cdot \text{H-DBTA}_2$ and $\text{Ca}[(R)\text{-1b}] \cdot \text{H-DBTA}_2$ Diastereomeric Complexes

Molecular features of the target guest molecules in the resolution experiments (*S*)-**1a** and (*R*)-**1b** have no unusual intramolecular bonding in their solid state forms (Figures 1 and 2). An analysis of intermolecular relations in the crystalline forms attests the formation of O-H...O donor...acceptor types of primary H-bridges. Such chains of H-bridges in (*S*)-**1a** and (*R*)-**1b** are produced in their chiral space groups $P2_1$ and $P2_12_12_1$.

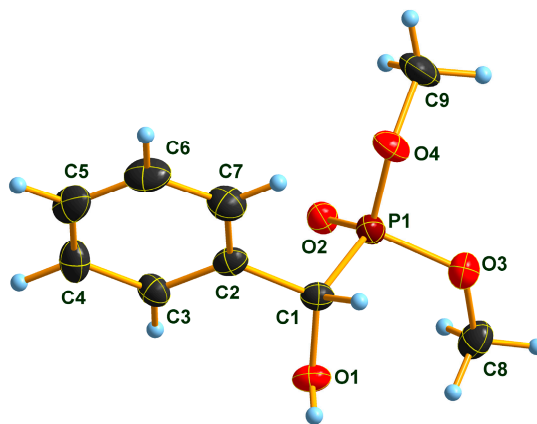


Figure 1. Molecular structure of compound (*S*)-**1a** in the crystal with thermal ellipsoids drawn at 50% probability level [41].

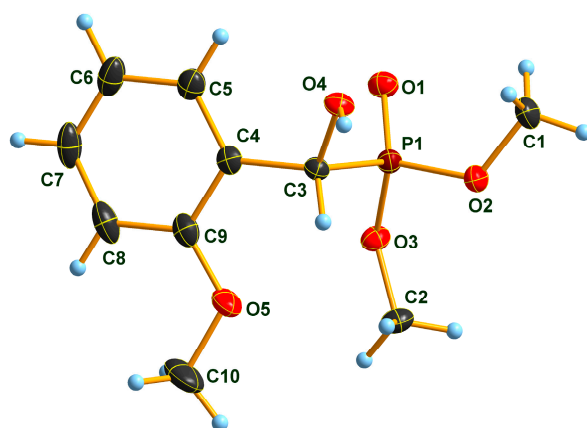


Figure 2. Molecular structure of compound (*R*)-**1b** in the crystal with thermal ellipsoids drawn at 50% probability level [41].

2.3. Sub-Units and Intermolecular Effects in $\text{Ca}[(S)\text{-1a} \bullet \text{H-DBTA}]_2$ and $\text{Ca}[(R)\text{-1b} \bullet \text{H-DBTA}]_2$ Diastereomeric Complexes

The much more complicated Ca-salt complexes are crystallizing in the same monoclinic $C2$ space group with the Ca^{2+} -cation sitting in special position on a crystallographic twofold rotor axis (Figures 3 and 4). Thus, the crystallographic asymmetric unit is made up from the half of the chemically sensible neutral (formally ‘molecular’) monomer unit. A further principal note comes from the analysis of the covalent linked molecules through coordination. Accordingly, these crystals are *catemer* (polymeric) structures having an infinite $1D$ -chain with $[0\ 1\ 0]$ base vector, i.e., chains propagated along the crystallographic b axes. A further peculiarity is of the C_2 -symmetric double-strand feature of these chains fused through the metal ions. From the point of view of the resolution from a racemate pool, we need to extend into the region of supramolecular interactions. As coordination is a basic vehicle in that too, this was analyzed in the first place.

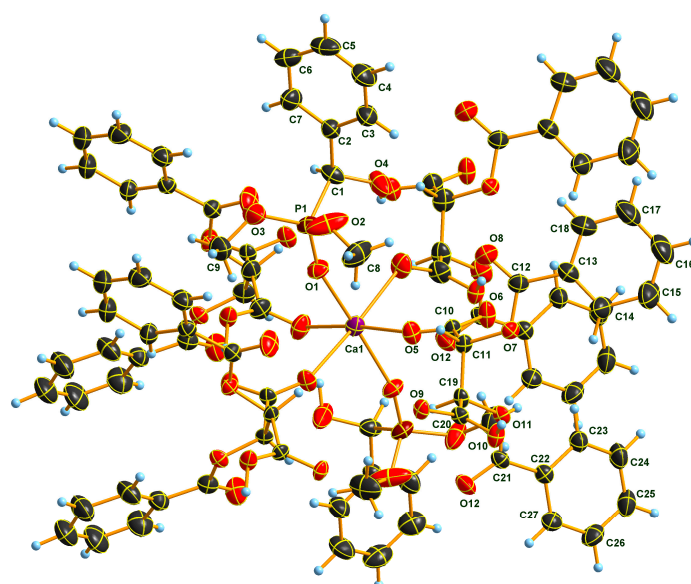


Figure 3. Molecular (monomer unit) structure of diastereomeric complex $\text{Ca}[(S)\text{-1a} \bullet \text{H-DBTA}]_2$ in the crystal with thermal ellipsoids drawn at 30% probability level. Unlabeled atoms are generated by the twofold crystallographic symmetry [41].

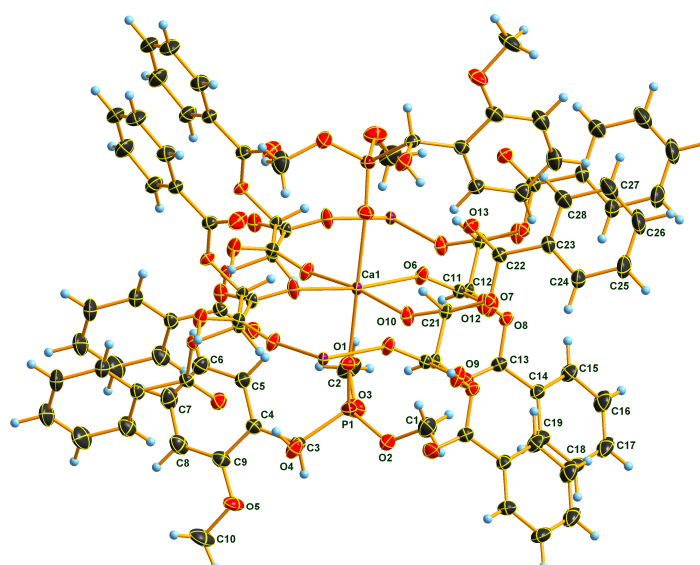


Figure 4. Molecular (monomer unit) structure of compound $\text{Ca}[(R)\text{-1b} \bullet \text{H-DBTA}]_2$ in the crystal with thermal ellipsoids drawn at 50% probability level. [41] Unlabeled atoms are generated by the twofold crystallographic symmetry.

2.4. Coordination in $\text{Ca}[(S)\text{-1a} \bullet \text{H-DBTA}]_2$ and $\text{Ca}[(R)\text{-1b} \bullet \text{H-DBTA}]_2$ Diastereomeric Complexes

The Ca^{2+} -cation coordination sphere is a square bipyramid polyhedron, as it was found earlier from similar resolution experiments [36,40]. The coordination sphere is composed such that two target resolute molecules O=P moieties are ligated in symmetric positions, while the square basal plane is made of 2-2 O atoms of the two ligating H-DBTA anions, one from the carboxylate, and the other from the carboxylic group. Figures 5 and 6 show some schematics of the coordinating polyhedron main features.

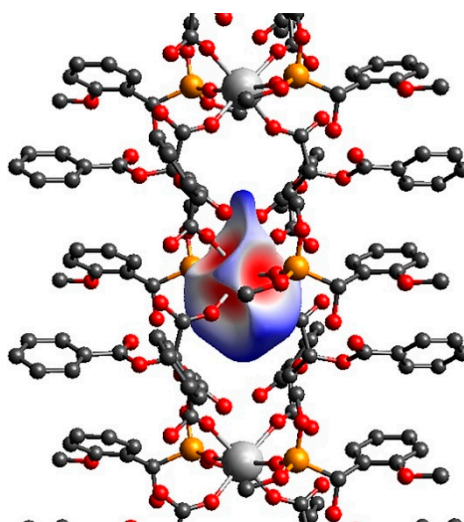


Figure 5. The Hirshfeld d_{norm} surface [42,43] of a central Ca-ion in a 3-molecule $\text{Ca}[(S)\text{-1a} \bullet \text{H-DBTA}]_2$ concatenated pile. Where Ca^{2+} links are shorter than the sum of the van der Waals radii the surface will be proportionally painted in red hue while the longer a contact is, the more blue the color will be and the contacts around the sum of van der Waals radii being white. H-atoms were omitted for clarity from this drawing.

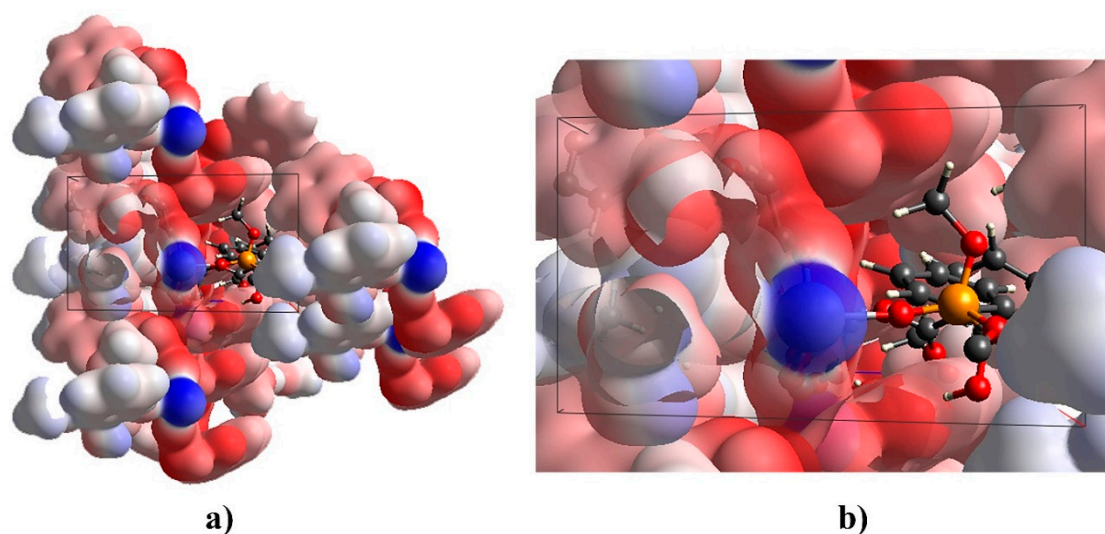


Figure 6. (a) Electrostatic potential colored surface [42,43] of the (S)-1a in the 3 salt complex; (b) inset from the same view; electrostatic potential (min/max values are -0.295 and 0.201 au.).

An ideally spherical (interaction-free) Hirshfeld-surface [42,43] is distorted into an asymmetric drop-like shape, while keeping the twofold symmetry. Distortions are due to coordination and also largely influenced by the asymmetry of the surrounding showing inherent direction dependence along the twofold axis direction (i.e., it is a polar axis). As directional senses of polar axes are physically different at the two ends of such an axis, they might exhibit dielectric polarization as e.g., in pyroelectric or piezoelectric crystals. Table 1 lists basic distances defining the coordination polyhedron in $\text{Ca}[(S)\text{-1a} \bullet \text{H-DBTA}]_2$ and $\text{Ca}[(R)\text{-1b} \bullet \text{H-DBTA}]_2$. The uniform and nearly unity quadratic elongation of 1.006 for 3 and 1.004 for 4 indicate formidable similarity and minimal distortions in the cation coordination [44,45]. These crystal structures apparently follow the four heuristic principles of Brown [46]. While a detailed comparison of the Ca–O distances between 3 and 4 makes little sense due to the largely differing experimental conditions (data collection temperature, crystal size, etc.), the tendency appears that Ca–O=P distances seem to be the shortest, while the tartarate O–Ca distances seem to be a little longer, and more or less alike. These data may in part reflect that other concurrent effects may operate in these environments.

Table 1. The coordination sphere distances $< 2.5 \text{ \AA}$ around the Ca-cation in 3* $[\text{Ca}[(S)\text{-1a} \bullet \text{H-DBTA}]_2]$ and in 4# $[\text{Ca}[(R)\text{-1b} \bullet \text{H-DBTA}]_2]$. O1 atoms are of the O=P groups, other O atoms come from the carboxyl–carboxylate moieties.

Atoms 3	3 $d_{(I,J)}$	4 $d_{(I,J)}$	Atoms 4
O(1)	2.2932(12)	2.284(3)	O(1)
O(1)c	2.2932(12)	2.284(3)	O(1)d
O(6)	2.3181(15)	2.324(4)	O(5)
O(6)c	2.3181(15)	2.324(4)	O(5)d
O(10)	2.2961(15)	2.331(4)	O(9)a
O(10)c	2.2961(15)	2.331(4)	O(9)b

Symmetry operators used on ligating O atoms in the respective crystals. $a = [x, -1+y, z]$; $b = [2-x, -1+y, 2-z]$; $c = [2-x, y, 1-z]$; $d = [2-x, y, 2-z]$. * Complex salt 3: quadratic elongation 1.006, angle variance $20.6(^{\circ})^2$. # Complex salt 4: quadratic elongation 1.004, angle variance $15.3(^{\circ})^2$.

2.5. Hydrogen Bonding in Diastereomeric Complexes 3 and 4

H-bonding may be one of these concurrent forces and is one of the responsible forces in molecular recognition events. The H-bonding system in the $\text{Ca}[(S)\text{-1a} \bullet \text{H-DBTA}]_2$ salt complex (Table 2) has some features linking the H-bridge active neutral OH–phosphonate moieties on one hand. This link is

realized in the form of the O4 ... O13 H-bridge of the OH-group to a benzyl-C=O. Here it appears also contributing to the molecular recognition event by the fixation of the α -OH group of the proper **1a** enantiomer in the cleft created by the Ca • H-DBTA environment. It is important to note here that while the principal binding of **1a** and **1b** are alike, there are a number of differences in the other weaker interactions. In the solid matrices of the Ca[(S)-**1a** • H-DBTA]₂ (**3**) and that of the Ca[(R)-**1b** • H-DBTA]₂ (**4**) crystals, these interactions are illustrated (c.f. Supplementary Figures S1 and S2) and briefly enumerated here on the basis of idealized covalent bonds of H-atoms. There is a short contact of 2.35 Å in α -hydroxyphosphonate **1a** within diastereomer **3** between the benzoyl C=O moiety and the H atom at the α C atom. The distance between the O atom of the α OH-group and an *ortho*-H of the phenyl group is 2.43 Å. This short intramolecular distance forms a coplanar pseudo 5-membered ring in **1a**. There is one more apparently short inter-stack H ... H contact (2.1 Å) between the two benzylic *ortho*-H atoms. The short distance pattern is different in diastereomeric complexes **4**. In contrast with **1a**, the C α H atom of hydroxyphosphonate **1b** is involved in an intramolecular close contact (2.26 Å) to the methoxy-O atom. In this manner, pseudo-5-membered ring is formed that is a coplanar with the phenyl moiety. As a consequence of this, the corresponding α H atom is no longer easily accessible. Thus, the molecular recognition is also aided by the benzyl aromatic ring linked to the same Ca-ion, such that it has a short *o*-C-H distance (3.09 Å) to the center of the phenyl moiety of **1b**. The third fixing directed interaction is established in this way. Another fixation of the phenyl group of **1b** comes from an interaction (3.17 Å) between a *para*-C-H and another benzyl ring center. In this way an infinite ... *o*-C-H --- ring-center/*p*-C-H --- ring-center/*o*-C-H ... cascade of interactions is formed.

Table 2. Potential O-H ... O hydrogen bond dimensions in the Ca[(S)-**1a** • H-DBTA]₂ salt complex with $d_{(D...A)} < R_{(D)} + R_{(A)} + 0.50$ and $d_{(H...A)} < R_{(H)} + R_{(A)} - 0.12$ Å and D-H ... A > 100.0°.

Donor—H	Acceptor	D-H (Å)	H ... A (Å)	D ... A (Å)	D-H ... A (°)
O(4)—H(4)	O(13) [il]	0.77(3)	2.04(3)	2.795(2)	166(3)
O(7)—H(70)	O(11)	1.07(4)	1.39(5)	2.445(2)	169(4)

Translation of ARU to equivalent positions. [il] = 2-x,y,1-z.

On the other hand, the second OH ... O type H-bridge stems from the H-DBTA mono-anions. These play a role of utmost importance from the point of views of both the resolution efficiency, and the construction of the crystalline matrix, as well as the completion of the coordination sphere. There are a number of possibilities of making the carboxylate-carboxyl H-bridge arrangements, all of which belong to the strongest O-H ... O type, albeit with only slightly varying O ... O distances between 2.44 and 2.54 Å [47]. The carboxylate-carboxyl H-bridges represent a further additional, in their own rights also catemer, motif shown in the COO⁻ - COOH form [47], too. Thus, the so formed polymeric double strand is not only fused through the metal ion coordination but is made even more stiff through this additional promoter-helper interaction.

Though the recognition cleft created by the Ca • H-DBTA environment cannot be visualized in situ, ample indirect a priori and a posteriori evidence point to its putative being an approximation somehow of the crystallization/selection stage. A reasonable impression how such a pocket might look like can be obtained, when we scrutinize the electrostatic-potential colored surface [42,43] of a selected portion of the **3** crystal structure (Figure 6). A naked **1a** molecule is seen oriented as to the optimal electrostatic conditions, as well as snugly steric fit is realized. The latter indicates that the important dispersion effects are also optimized in that environment, as alluded to the fitting of apolar components earlier. That such rigid framework may exist in concentrated solutions in metastable states around the precipitation conditions in the form of not only the metal-ion bound tartrate anion but also of the strong hydrogen-bond to the anionic O-atom is made probable also when considering dielectric [48,49] and other properties of the 2-butanone (MEK) solvent used in the crystallization experiment. Among other features MEK is known to have moderate relative permittivity aiding in sustaining cationic-anionic association, as well as strong ionic H-bridges. A high dielectric constant media (such as formamide,

water, or DMSO) may be more harmful for such a basically ionic assembly by promoting isolation of the cationic and the anionic components from each other. MEK may coordinate to the cation as well. Nevertheless, this solvent is a much weaker competitor against **1a** as it lacks at least two strong interactions, and MEK is not that efficient isolation media either. It seems that the system of these crystal structures provides at least a partly rational basis for the explanation of the preference and success of the hemi-acid-Ca salts for the resolution of optically active hydroxyphosphonates.

3. Conclusions

The optical resolution of two dimethyl α -hydroxy-arylmethylphosphonates (aryl = Ph and 2-MeOPh) was elaborated via diastereomer complex formation using the acidic calcium salt of *O,O'*-dibenzoyl-(2*R*,3*R*)-tartaric acid as the resolving agent. After purification and decomposition of the corresponding diastereomers, the major enantiomer (*S* and *R*, respectively) of the α -hydroxyphosphonates were obtained with enantiomeric excess values of 96% and 68%, respectively. Structures of the two diastereomeric complexes and the two α -hydroxy-arylmethylphosphonates were evaluated by single crystal X-ray measurements. Detailed study on the X-ray structures allowed conclusions on the intermolecular interactions operating in the complexes, and on the *H*-bonding. The high *ee* values may be derived from the concerted effects of the intricate combinations of the 3D-effects of directed electrostatic forces involving those from ionic, as well as from neutral *H*-bridges and less directional polarization effects manifested in steric fit and interactions. All these are resulting from a multitude of assembled molecules at a rather early stage of crystal growth.

4. Experimental

The ratio of the α -hydroxyphosphonate and the resolving agent was determined by ^1H NMR on a Bruker DRX 500 instrument operating at 500 MHz.

The enantiomeric excess (*ee*) values were determined by chiral HPLC on a PerkinElmer Series 200 instrument equipped with chiral HPLC using Kromasil[®] 5 μm Amycoat or Phenomenex Lux[®] Amylose-2 5 μm column (250 \times 4.6 mm ID, hexane/ethanol 85:15 as an eluent with a flow rate of 0.8 mL/min, *T* = 20 $^\circ\text{C}$, UV detector λ = 254 nm). Retention times: 9.9 min for (*S*)-**1a**, 12.3 min for (*R*)-**1a** (Kromasil[®] 5 μm Amycoat column); 14.9 min for (*R*)-**1b** and 16.8 min for (*S*)-**1b** (Phenomenex Lux[®] Amylose-2 5 μm column).

Racemic α -hydroxyphosphonates (**1a** and **1b**) [39] and resolving agent $\text{Ca}(\text{H-DBTA})_2$ (**2**) [40] were prepared according to procedures reported by us.

4.1. Single Crystal X-Ray Diffraction Studies of Optically Active α -Hydroxyphosphonates (*S*)-**1a** and (*R*)-**1b** as Well as of the Diastereomeric Complex $\text{Ca}[(\text{R})\text{-1b} \bullet \text{H-DBTA}]_2$

Single crystals of compound (*S*)-**1a**, (*R*)-**1b** and $\text{Ca}[(\text{R})\text{-1b} \bullet \text{H-DBTA}]_2$ suitable for X-ray diffraction, were obtained by slow evaporation of the respective acetone solutions. The crystals were introduced into perfluorinated oil and a suitable single crystal was carefully mounted on the top of a thin glass fiber. Data collection were performed with an Oxford Xcalibur 3 diffractometer using the CrysAlisPro software [50]. Absorption correction using the multiscan method [50] was applied. The structures were solved with SHELXS-97 [51], refined with SHELXL-97 [52] and finally checked using PLATON [53].

4.2. Single Crystal X-Ray Diffraction Studies of Diastereomeric Complex $\text{Ca}[(\text{S})\text{-1a} \bullet \text{H-DBTA}]_2$

Single crystals of compound $\text{Ca}[(\text{S})\text{-1a} \bullet (\text{H-DBTA})]_2$, suitable for X-ray diffraction, were obtained and treated as of the other three compounds. Data collection was performed with a Bruker D8 Venture diffractometer equipped with a Bruker D8 Venture TXS rotating anode X-ray tube using the Bruker Instrument Service software [54], SAINT software [55] was used for data reduction. Absorption correction using multiscan method within the SADABS software [56] was applied. The structure was solved with SHELXS-97 [51], refined with SHELXL-97 [52], and finally checked using PLATON [53]. Details for data collection and structure refinement are summarized in the Supplementary Materials.

Essential crystallographic data and model coordinates for **1a/4** were deposited with the Cambridge Crystallographic Data Centre and are accessible under the CCDC Deposition Numbers 1990880–1990883 at <https://www.ccdc.cam.ac.uk/structures>.

4.3. Procedure for the Preparation of Optically Active $\text{Ca}[(S)\text{-1a} \bullet \text{H-DBTA}]_2$ Complex and Its Single Crystals

A mixture of 3.8 mmol (0.81 g) of dimethyl 1-hydroxy-1-phenylmethylphosphonate (**1a**) and 0.95 mmol (0.71 g) of $\text{Ca}(\text{H-DBTA})_2$ was dissolved in 3.0 mL of methyl ethyl ketone at reflux. After the solution became clear, it was allowed to cool to 26 °C. After stirring for 24 h at 26 °C, the crystalline diastereomeric complex was filtered, and it was washed with 1.5 mL of methyl ethyl ketone to give 0.51 g (yield = 46%) of $\text{Ca}[(S)\text{-1a} \bullet \text{H-DBTA}]_2$ with a diastereomeric excess of 47%. The diastereomeric complex was purified by crystallization: 3.0 mL of methyl ethyl ketone was added to the diastereomeric complex and the suspension was heated at reflux until it became clear. The solution was allowed to cool to 26 °C and it was stirred for 24 h at 26 °C. Filtration of the crystalline diastereomeric complex afforded 0.35 g (yield = 31%) of $\text{Ca}[(S)\text{-1a} \bullet \text{H-DBTA}]_2$ with a diastereomeric excess of 96%. Then, 4.2 μmol (5.0 mg) of the diastereomeric complex obtained was dissolved in 40 μL of acetone. The solvent was allowed to evaporate slowly to give single crystals of $\text{Ca}[(S)\text{-1a} \bullet \text{H-DBTA}]_2$.

4.4. Procedure for the Preparation of Optically Active $(S)\text{-1a}$ and Its Single Crystals

To 0.35 g of $\text{Ca}[(S)\text{-1a} \bullet \text{H-DBTA}]_2$ (*de* = 96%) prepared according to the method shown above, 20.0 mL of 5 m/m% NaHCO_3 solution was added. The aqueous phase was extracted with 4×20.0 mL of dichloromethane to afford 0.11 g (yield = 28%) of $(S)\text{-1a}$ with an enantiomeric excess of 96%. Then, 0.02 mmol (5.0 mg) of $(S)\text{-1a}$ so obtained was dissolved in 40 μL of acetone. The solvent was allowed to evaporate slowly to give single crystals of $(S)\text{-1a}$.

4.5. Procedure for the Preparation of Optically Active $\text{Ca}[(R)\text{-1b} \bullet \text{H-DBTA}]_2$ Complex and Its Single Crystals

A mixture of 0.50 mmol (0.12 g) of dimethyl 1-hydroxy-1-(2-methoxyphenyl)methylphosphonate and 0.13 mmol (0.09 g) of $\text{Ca}(\text{H-DBTA})_2$ was dissolved in 0.30 mL of benzyl alcohol under reflux. After the solution became clear, it was allowed to cool to 26 °C. After stirring for 24 h at 26 °C, the crystalline diastereomeric complex was filtered, and it was washed with 0.20 mL of benzyl alcohol to give 0.15 g (yield = 99%) of $\text{Ca}[(R)\text{-1b} \bullet \text{H-DBTA}]_2$ with a diastereomeric excess of 68%. Then, 4.0 μmol (5.0 mg) of the diastereomeric complex obtained was dissolved in 40 μL of acetone. The solvent was allowed to evaporate slowly to give single crystals of $\text{Ca}[(R)\text{-1b} \bullet \text{H-DBTA}]_2$.

4.6. Procedure for the Preparation of Optically Active $(R)\text{-1b}$ and Its Single Crystals

A mixture of 8.7 mmol (2.1 g) of dimethyl 1-hydroxy-1-(2-methoxyphenyl)methylphosphonate and 2.2 mmol (1.6 g) of $\text{Ca}(\text{H-DBTA})_2$ was dissolved in 40.0 mL of ethyl acetate at reflux. After the solution became clear, it was allowed to cool to 26 °C. After standing 3 h at 26 °C, the crystallized diastereomeric complex was filtered out and was washed with 20.0 mL of ethyl acetate to give 1.6 g (yield = 62%) of $\text{Ca}[(R)\text{-1b} \bullet \text{H-DBTA}]_2$ with a diastereomeric excess of 60%. The diastereomeric complex was purified by two recrystallization steps from 40.0 and 15.0 mL of ethyl acetate, respectively. For the recrystallization, the diastereomeric complex was dissolved in ethyl acetate on heating, then the solution was allowed to cool to 26 °C. After 3 h of stirring, the crystalline diastereomeric complex was filtered to afford eventually 0.99 g (yield = 39%) of $\text{Ca}[(R)\text{-1b} \bullet \text{H-DBTA}]_2$ with a diastereomeric excess of 68%. Then, 70.0 mL of 5 m/m% NaHCO_3 solution was added to the diastereomeric complex and the aqueous phase was extracted with 4×70.0 mL of dichloromethane to afford 0.34 g (yield = 34%) of $(R)\text{-1b}$ with an enantiomeric excess of 68%. Finally, 0.02 mmol (5.0 mg) of $(R)\text{-1b}$ obtained was dissolved in 40 μL of acetone. The solvent was allowed to evaporate slowly to give single crystals of $(R)\text{-1b}$.

Supplementary Materials: The following are available online at <http://www.mdpi.com/2073-8994/12/5/758/s1>.

Author Contributions: Projekt management, funding, writing the ms, G.K.; planning and performing the preparative experiments, writing the ms, P.B. and Z.R.; single crystal X-ray structure determinations and refinements, data processing and documentations, M.C.: single crystal structure analyses, writing up the X-ray results, K.K. All authors have read and agreed to the published version of the manuscript.

Funding: This project was supported by the National Research, Development and Innovation Office (K119202). M.C. acknowledges the Hungarian Pension Fund for support to this work.

Conflicts of Interest: The authors declare no conflict of interest.

References

1. Patel, D.V.; Rielly-Gauvin, K.; Ryono, D.E.; Free, C.A.; Rogers, W.L.; Smith, S.A.; DeForrest, J.M.; Oehl, R.S.; Petrillo, E.W. Alpha-hydroxy phosphinyl-based inhibitors of human renin. *J. Med. Chem.* **1995**, *38*, 4557–4569. [[CrossRef](#)]
2. Song, H.; Mao, H.; Shi, D. Synthesis and herbicidal activity of α -hydroxy phosphonate derivatives containing pyrimidine moiety. *Chin. J. Chem.* **2010**, *28*, 2020–2024. [[CrossRef](#)]
3. Pokalwar, R.U. Synthesis and antibacterial activities of α -hydroxyphosphonates and α -acetyloxyphosphonates derived from 2-chloroquinoline-3-carbaldehyde. *Arkivoc* **2006**, 196. [[CrossRef](#)]
4. Kategaonkar, A.H.; Pokalwar, R.U.; Sonar, S.S.; Gawali, V.U.; Shingate, B.B.; Shingare, M.S. Synthesis, in vitro antibacterial and antifungal evaluations of new α -hydroxyphosphonate and new α -acetoxyphosphonate derivatives of tetrazolo [1, 5-a] quinoline. *Eur. J. Med. Chem.* **2010**, *45*, 1128–1132. [[CrossRef](#)]
5. Sampath, C.; Raju, C.N.; Rao, C.V. An efficient synthesis, spectral characterization, anti-microbial and anti-oxidant activities of novel α -hydroxyphosphonates and α -hydroxyphosphinates. *Phosphorus Sulfur Silicon Relat. Elem.* **2015**, *191*, 95–99. [[CrossRef](#)]
6. Rádai, Z.; Windt, T.; Nagy, V.; Füredi, A.; Kiss, N.Z.; Randelovic, I.; Tóvári, J.; Keglevich, G.; Szakács, G.; Tóth, S. Synthesis and anticancer cytotoxicity with structural context of an α -hydroxyphosphonate based compound library derived from substituted benzaldehydes. *New J. Chem.* **2019**, *43*, 14028–14035. [[CrossRef](#)]
7. Kalla, R.M.N.; Lee, H.R.; Cao, J.; Yoo, J.-W.; Kim, I. Phospho sulfonic acid: An efficient and recyclable solid acid catalyst for the solvent-free synthesis of α -hydroxyphosphonates and their anticancer properties. *New J. Chem.* **2015**, *39*, 3916–3922. [[CrossRef](#)]
8. Blaser, H.-U. Chirality and its implications for the pharmaceutical industry. *Rend. Fis. Acc. Lincei* **2013**, *24*, 213–216. [[CrossRef](#)]
9. Nguyen, L.A.; He, H.; Pham-Huy, C. Chiral drugs: An overview. *Int. J. Biomed. Sci.* **2006**, *2*, 85–100.
10. Gröger, H.; Vogl, E.M.; Shibasaki, M. New catalytic concepts for the asymmetric aldol reaction. *Chem. Eur. J.* **1998**, *4*, 1137–1141. [[CrossRef](#)]
11. Kolodiazhnyi, O.I. Chiral hydroxy phosphonates: Synthesis, configuration and biological properties. *Russ. Chem. Rev.* **2006**, *75*, 227–253. [[CrossRef](#)]
12. Kolodiazhnyi, O. Asymmetric synthesis of hydroxyphosphonates. *Tetrahedron Asymmetry* **2005**, *16*, 3295–3340. [[CrossRef](#)]
13. Kolodyazhnaya, A.O.; Kukhar, V.P.; Kolodyazhnyi, O.I. Organic catalysis of phospho-aldol condensation. *Russ. J. Gen. Chem.* **2008**, *78*, 2043–2051. [[CrossRef](#)]
14. Hirashima, S.-I.; Arai, R.; Nakashima, K.; Kawai, N.; Kondo, J.; Koseki, Y.; Miura, T. Asymmetric hydrophosphonylation of aldehydes using a cinchona-diaminomethylenemalononitrile organocatalyst. *Adv. Synth. Catal.* **2015**, *357*, 3863–3867. [[CrossRef](#)]
15. Uraguchi, D.; Ito, T.; Ooi, T. Generation of chiral phosphonium dialkyl phosphite as a highly reactive P-nucleophile: Application to asymmetric hydrophosphonylation of aldehydes. *J. Am. Chem. Soc.* **2009**, *131*, 3836–3837. [[CrossRef](#)]
16. Abell, J.P.; Yamamoto, H. Catalytic enantioselective Pudovik reaction of aldehydes and aldimines with tethered bis(8-quinolinato) (TBOx) aluminum complex. *J. Am. Chem. Soc.* **2008**, *130*, 10521–10523. [[CrossRef](#)]
17. Deng, T.; Cai, C. Bis(oxazoline)-copper catalyzed enantioselective hydrophosphonylation of aldehydes. *RSC Adv.* **2014**, *4*, 27853–27856. [[CrossRef](#)]
18. Muthupandi, P.; Sekar, G. Synthesis of an unusual dinuclear chiral iron complex and its application in asymmetric hydrophosphorylation of aldehydes. *Org. Biomol. Chem.* **2012**, *10*, 5347. [[CrossRef](#)]

19. Sun, L.; Guo, Q.-P.; Li, X.; Zhang, L.; Li, Y.-Y.; Da, C.-S. C₂-symmetric homobimetallic zinc complexes as chiral catalysts for the highly enantioselective hydrophosphonylation of aldehydes. *Asian J. Org. Chem.* **2013**, *2*, 1031–1035. [[CrossRef](#)]
20. Guin, J.; Wang, Q.; van Gemmeren, M.; List, B. The catalytic asymmetric abramov reaction. *Angew. Chem. Int. Ed.* **2015**, *54*, 355–358. [[CrossRef](#)]
21. Goulioukina, N.S.; Bondarenko, G.N.; Bogdanov, A.V.; Gavrilov, K.N.; Beletskaya, I.P. Asymmetric hydrogenation of α -keto phosphonates with chiral palladium catalysts. *Eur. J. Org. Chem.* **2009**, 510–515. [[CrossRef](#)]
22. Nesterov, V.; Kolodiazhnyi, O. New method for the asymmetric hydroboration of ketophosphonates and the synthesis of phospho-carnitine. *Tetrahedron Asymmetry* **2006**, *17*, 1023–1026. [[CrossRef](#)]
23. Nesterov, V.; Kolodiazhnyi, O. New method for the asymmetric reduction of ketophosphonates. *Phosphorus Sulfur Silicon Relat. Elem.* **2008**, *183*, 687–688. [[CrossRef](#)]
24. Skropeta, D.; Schmidt, R.R. Chiral, non-racemic α -hydroxyphosphonates and phosphonic acids via stereoselective hydroxylation of diallyl benzylphosphonates. *Tetrahedron Asymmetry* **2003**, *14*, 265–273. [[CrossRef](#)]
25. Pogatchnik, D.M.; Wiemer, D.F. Enantioselective synthesis of α -hydroxy phosphonates via oxidation with (camphorsulfonyl)oxaziridines. *Tetrahedron Lett.* **1997**, *38*, 3495–3498. [[CrossRef](#)]
26. Kafarski, P.; Lejczak, B. Application of bacteria and fungi as biocatalysts for the preparation of optically active hydroxyphosphonates. *J. Mol. Catal. B Enzym.* **2004**, *29*, 99–104. [[CrossRef](#)]
27. Pàmies, O.; Bäckvall, J.-E. An efficient route to chiral α - and β -hydroxyalkanephosphonates. *J. Org. Chem.* **2003**, *68*, 4815–4818. [[CrossRef](#)]
28. Li, Y.-F.; Hammerschmidt, F. Enzymes in organic chemistry, part 1: Enantioselective hydrolysis of α -(acyloxy)phosphonates by esterolytic enzymes. *Tetrahedron Asymmetry* **1993**, *4*, 109–120. [[CrossRef](#)]
29. Demizu, Y.; Moriyama, A.; Onomura, O. Nonenzymatic kinetic resolution of racemic α -hydroxyalkanephosphonates with chiral copper catalyst. *Tetrahedron Lett.* **2009**, *50*, 5241–5244. [[CrossRef](#)]
30. Kaboudin, B.; Alavi, S.; Kazemi, F.; Aoyama, H.; Yokomatsu, T. Resolution of racemic α -hydroxyphosphonates: bi(OTF)₃-catalyzed stereoselective esterification of α -hydroxyphosphonates with (+)-dibenzoyl-l-tartaric anhydride. *ACS Omega* **2019**, *4*, 15471–15478. [[CrossRef](#)]
31. Rádai, Z.; Kiss, N.Z.; Czugler, M.; Karaghiosoff, K.; Keglevich, G. The typical crystal structures of a few representative α -aryl- α -hydroxyphosphonates. *Acta Crystallogr. Sect. C Struct. Chem.* **2019**, *75*, 283–293. [[CrossRef](#)]
32. Bagi, P.; Ujj, V.; Czugler, M.; Fogassy, E.; Keglevich, G. Resolution of P-stereogenic P-heterocycles via the formation of diastereomeric molecular and coordination complexes (a review). *Dalton Trans.* **2016**, *45*, 1823–1842. [[CrossRef](#)]
33. Bagi, P.; Varga, B. Preparation of enantiomerically enriched P-stereogenic dialkyl-arylphosphine oxides via coordination mediated optical resolution. *Symmetry* **2020**, *12*, 215.
34. Bagi, P.; Varga, B.; Szilágyi, A.; Karaghiosoff, K.; Czugler, M.; Fogassy, E.; Keglevich, G. The resolution of acyclic P-stereogenic phosphine oxides via the formation of diastereomeric complexes: A case study on ethyl-(2-methylphenyl)-phenylphosphine oxide. *Chirality* **2018**, *30*, 509–522. [[CrossRef](#)]
35. Mravik, A.; Böcskei, Z.; Simon, K.; Elekes, F.; Izsáki, Z. Chiral recognition of alcohols in the crystal lattice of simple metal complexes of O,O'-dibenzoyltartaric Acid: Enantiocomplementarity and simultaneous resolution. *Chem. Eur. J.* **1998**, *4*, 1621–1627. [[CrossRef](#)]
36. Mravik, A.; Böcskei, Z.; Katona, Z.; Markovits, I.; Pokol, G.; Menyhárd, D.K.; Fogassy, E. A new optical resolution method: Coordinative resolution of mandelic acid esters. The crystal structure of calcium hydrogen (2R,3R)-O,O'-dibenzoyl tartrate-2(R)-(-)-methyl mandelate. *Chem. Commun.* **1996**, 1983–1984. [[CrossRef](#)]
37. Mravik, A.; Böcskei, Z.; Katona, Z.; Markovits, I.; Fogassy, E. Coordination-mediated optical resolution of carboxylic acids with O, O'-dibenzoyltartaric acid. *Angew. Chem. Int. Ed.* **1997**, *36*, 1534–1536. [[CrossRef](#)]
38. Yang, B.; Xie, H.; Ran, K.; Gan, Y. Efficient synthesis and resolution of tenofovir alafenamide. *Lett. Org. Chem.* **2017**, *15*, 10–14. [[CrossRef](#)]
39. Keglevich, G.; Rádai, Z.; Kiss, N.Z. To date the greenest method for the preparation of α -hydroxyphosphonates from substituted benzaldehydes and dialkyl phosphites. *Green Process. Synth.* **2017**, *6*, 197–201. [[CrossRef](#)]

40. Ujj, V.; Schindler, J.; Novák, T.; Czugler, M.; Fogassy, E.; Keglevich, G. Coordinative resolution of 1-phenyl- and 1-naphthyl-3-methyl-3-phospholene 1-oxides with calcium hydrogen O,O'-dibenzoyl-(2R,3R)-tartrate or calcium hydrogen O,O'-di-p-toluyyl-(2R,3R)-tartrate. *Tetrahedron Asymmetry* **2008**, *19*, 1973–1977. [CrossRef]
41. Putz, H.; Brandenburg, K. Diamond—Crystal and Molecular Structure Visualization. *Cryst. Impact-Gbr Kreuzherrenstr.* **2006**, *102*, 53227.
42. McKinnon, J.; Spackman, M.A.; Mitchell, A.S. Novel tools for visualizing and exploring intermolecular interactions in molecular crystals. *Acta Crystallogr. Sect. B Struct. Sci.* **2004**, *60*, 627–668. [CrossRef]
43. Spackman, M.A.; Jayatilaka, D. Hirshfeld surface analysis. *Cryst. Eng. Comm.* **2009**, *11*, 19–32. [CrossRef]
44. Robinson, K.; Gibbs, G.V.; Ribbe, P.H. Quadratic elongation: A quantitative measure of distortion in coordination polyhedra. *Science* **1971**, *172*, 567–570. [CrossRef]
45. Brown, I.D. On measuring the size of distortions in coordination polyhedra. *Acta Crystallogr. Sect. B Struct. Sci.* **2006**, *62*, 692–694. [CrossRef]
46. Brown, I.D. Recent developments in the methods and applications of the bond valence model. *Chem. Rev.* **2009**, *109*, 6858–6919. [CrossRef]
47. D'Ascenzo, L.; Auffinger, P. A comprehensive classification and nomenclature of carboxyl-carboxyl(ate) supramolecular motifs and related catemers: Implications for biomolecular systems. *Acta Crystallogr. Sect. B Struct. Sci. Cryst. Eng. Mater.* **2015**, *71*, 164–175. [CrossRef]
48. Sudake, Y.; Kamble, S.; Patil, S.; Khirade, P.; Mehrotra, S. Study of dynamics of allyl chloride-2-butanone binary system using time domain reflectometry. *J. Korean Chem. Soc.* **2012**, *56*, 20–27. [CrossRef]
49. Common Solvents Used in Organic Chemistry: Table of Properties. 2016. Available online: https://www.organicdivision.org/wp-content/uploads/2016/12/organic_solvents.html (accessed on 10 February 2020).
50. Program Package CrysAlisPro 1.171.39.46e (Rigaku OD). 2018. Available online: <http://www.rsc.org/suppdata/c8/tc/c8tc04867c/c8tc04867c1.pdf> (accessed on 10 February 2020).
51. Sheldrick, G.M. *SHELXS-97: Program for Crystal Structure Solution*; University of Göttingen: Göttingen, Germany, 1997.
52. Sheldrick, G.M. *SHELXL-97: Program for the Refinement of Crystal Structures*; University of Göttingen: Göttingen, Germany, 1997.
53. Spek, A.L. *PLATON: A Multipurpose Crystallographic Tool*; Utrecht University: Utrecht, The Netherlands, 1999.
54. Bruker Instrument Service v3.0.21. Available online: <https://www.bruker.com/products/x-ray-diffraction-and-elemental-analysis/single-crystal-x-ray-diffraction/sc-xrd-software/apex3.html> (accessed on 1 April 2020).
55. SAINT V8.18C (Bruker AXS Inc.). 2011. Available online: <https://www.bruker.com/products/x-ray-diffraction-and-elemental-analysis/single-crystal-x-ray-diffraction/sc-xrd-software/apex3.html> (accessed on 1 April 2020).
56. SADABS-2016/2. Available online: <https://www.bruker.com/products/x-ray-diffraction-and-elemental-analysis/single-crystal-x-ray-diffraction/sc-xrd-software/apex3.html> (accessed on 1 April 2020).

